



ELSEVIER

Contents lists available at [ScienceDirect](https://www.sciencedirect.com)

Comptes rendus - Geoscience

www.journals.elsevier.com/comptes-rendus-geoscience

Petrology, Geochemistry (Mineralogy)

The intermediate step in fractionation trends of mildly alkaline volcanic suites: An experimental insight from the Pavin trachyandesite (Massif Central, France)



Morgane Rondet, Caroline Martel*, Jean-Louis Bourdier

Institut des sciences de la Terre d'Orléans (ISTO), Université d'Orléans–CNRS–BRGM, Orléans, France

ARTICLE INFO

Article history:

Received 27 July 2018

Accepted 25 July 2019

Available online 9 October 2019

Handled by Bruno Scaillet

Keywords:

Trachyandesite

Pavin

Experimental petrology

Differentiation

ABSTRACT

We examined magma storage conditions and eruptive dynamics for the trachyandesite (~58 wt% SiO₂, 9–10 wt% alkalis) of the Pavin monogenetic volcano, a maar-like explosive crater belonging to a small group of youngest volcanoes in the Massif Central. By confronting the natural samples to experimental products, we constrained pre-eruptive conditions around 950–975 °C, 150–200 MPa (~5.5–7.0 km in depth), NNO+1.5, and 4.5–5.5 wt% melt H₂O. There is petrological evidence of magma crystallization in the conduit up to shallow levels (~50 MPa; 2 km in depth) before fragmentation into pumice clasts in the last kilometre of ascent. The experiments highlight the role of biotite and of crystallization pressure in defining separate compositional trends of residual liquids, i.e. alkaline (trachytes) versus sub-alkaline (dacite-rhyolite).

© 2019 Académie des sciences. Published by Elsevier Masson SAS. This is an open access article under the CC BY-NC-ND license (<http://creativecommons.org/licenses/by-nc-nd/4.0/>).

1. Introduction

The Tertiary to Quaternary volcanic province of the Massif Central (France) is part of an intraplate alkaline volcanism, the Cenozoic European Volcanic Province (CEVP) that spreads from Spain to Poland and is spatially associated with a large-scale rift system surrounding the Alpine orogen. Rifting and volcanism globally formed due to local extension and mantle upwelling in response to the Alpine orogeny (Lustrino and Wilson, 2007, and references therein). In the Massif Central, discrete volcanic fields are recognized based on spatiotemporal criteria, ranging in age mostly from the middle Miocene to the Holocene. Most of those fields are uniquely basaltic, while some erupted magmas of intermediate compositions, i.e. trachyandesites *s.l.* and/or phonolites, along with subordinate volumes of trachytes (Velay, Cantal, Chaîne des Puys) and even

rhyolites (Monts Dore) (e.g., Brousse, 1961; Downes, 1987). Comparable alkaline suites with differentiated terms have been documented in other segments of the CEVP, notably the Upper Rhine Valley (e.g., Schreiber et al., 1999; Wörner et al., 1983), and the Bohemian Massif (Ackerman et al., 2015; Ulrych et al., 1999). The differentiated terms of the CEVP suites have been largely interpreted as resulting from polybaric differentiation of variously silica under-saturated primary mafic magmas by assimilation-fractional crystallization (AFC) processes ending in the upper crust. Such a case has been made for the Massif Central magmatic suites: Cantal (Downes, 1984; Wilson et al., 1995), Monts Dore (Briot et al., 1991), and Velay and Chaîne des Puys (Maury et al., 1980; Villemant et al., 1980, 1981). Crystal fractionation trends in those suites have been defined mainly from the mineral assemblages of the various terms of the suites, and on mass-balance calculations using major and trace elements. However, constraints by phase-equilibrium experiments on the storage conditions and fractionation paths of such mildly alkaline, intermediate, and silicic magmas remain currently scarce. A previous experimental study

* Corresponding author.

E-mail addresses: cmartel@cnrs-orleans.fr, caroline.martel@cnrs-orleans.fr (C. Martel).

(Martel et al., 2013) investigated the storage conditions of trachytic magmas from the youngest volcanic field in the Massif Central, i.e. the partly Holocene Chaîne des Puys. In the present paper, we go back to an intermediate step in the differentiation trend by examining phase-equilibrium conditions for a representative trachyandesite (~58 wt% SiO₂) taken from the neighbouring Holocene Pavin volcano. Pavin is a maar-like explosive crater belonging to a small group of youngest volcanoes in the Massif Central, i.e. slightly younger than the Chaîne des Puys volcanoes, and located only about 40 km south of them in a similar tectonic setting. The aim of this study is (1) to constrain the storage conditions of the Pavin trachyandesite, erupted from a likely small-volume reservoir; (2) to investigate the conditions that can generate trachytic liquids (such as those of the Chaîne des Puys) from a trachyandesitic parent by crystal fractionation.

2. Geological setting and sampling

The Pavin volcano is a roughly circular explosive crater 900–1000 m in diameter, filled by a crater lake about 750 m in diameter and 92 m in depth at most. The crater rim crosscuts lava flows from an adjacent scoria cone, the Montchal volcano. Four kilometres south stands another morphologically well-preserved scoria cone, the Montcineyre volcano. At least one neighbouring maar, Estivadoux, is demonstrated by typical phreatomagmatic basaltic

deposits exposed in its surroundings, though it is currently buried by Montchal scoria flows and proximal Pavin deposits. Therefore, Pavin belongs to a small group of at least four recent monogenetic volcanoes (the Pavin group herein; Fig. 1), whose tephrostratigraphical and field relationships unambiguously define the relative eruption chronology as Montcineyre–Estivadoux–Montchal–Pavin, from the oldest to the youngest (Bourdier, 1980). The lack of paleosol and the erosive contact between tephra layers from those volcanoes strongly suggest eruption within a short period of time. The most recent radiometric assessment gives an age of 4720 ± 170 B. (current age of 6730 ± 170) for the Pavin eruption, and a time elapse of 100–700 years between the oldest (Montcineyre) and youngest (Pavin) eruptions (Juvigné and Miallier, 2016). So far, no volcanic eruption in the Massif Central has been dated younger than the Pavin one, nor any unequivocal tephra has been recovered above the Pavin one, so that Pavin currently stands as the youngest volcano in continental France (Juvigné and Miallier, 2016).

Pavin is located only about 40 km south of the southernmost volcano of the Chaîne des Puys, a monogenetic field of about 80 volcanoes, mostly scoria cones, forming a north–south-trending chain about 30 km long, west of the city of Clermont-Ferrand. The Chaîne des Puys volcanoes range in age from less than 100 000 to about 6000–7000 years. The Pavin volcanic group is thus close in age to of the youngest volcanoes of the Chaîne des Puys. Both

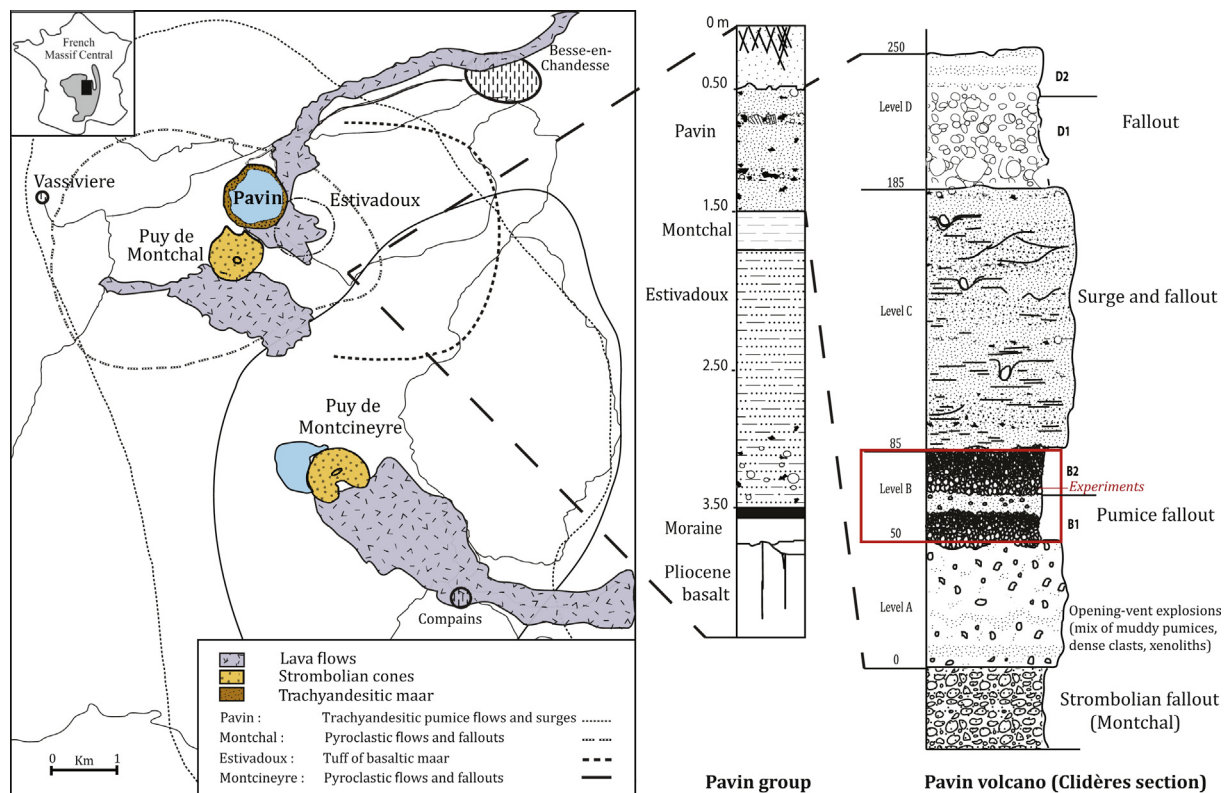


Fig. 1. Localization of the Pavin group (modified after Bourdier, 1980), Pavin group simplified stratigraphic sequence (modified after Boivin et al., 2009), and the Pavin volcano stratigraphic sequence at Clidères outcrop showing the fallout level (basis of B2) where pumices have been sampled for the experiments.

monogenetic fields occur in the same tectonic setting, in which the location of eruptive vents is mainly controlled by regional faults dating from the Variscan orogeny and rejuvenated during the post-Alpine rifting episode. In those respects, the Pavin group could be viewed as a southern extension of the larger Chaîne des Puys volcanic field (Boivin et al., 2009).

The Pavin proximal pyroclastic deposits (Boivin et al., 2010; Bourdier, 1980; Camus et al., 1973; Leyrit et al., 2016) have juvenile components consisting of dominant macroscopically homogeneous, yellowish-weathering pumices, and subordinate greyish, denser clasts and texturally heterogeneous pumices (Arbaret and Bourdier, 2018). All textural types are distinctively amphibole–phyric and display similar mineralogy and bulk-rock composition (Bourdier, 1980; Villemant et al., 2016). The juvenile magma is a mildly alkaline (peralkalinity index, P.I. = 0.6–0.8) trachyandesite (or benmoreite) (~58 wt% SiO₂; Table 1, Fig. 2). In the Pavin group, the Montcineyre and Estivadoux magmas are nepheline-normative alkaline basalts to basanites and the Montchal one is a trachybasalt (or hawaiite). Thus, the Pavin magma is the most differentiated (Bourdier, 1980). Previous petrological and geochemical studies

have linked the magma compositions of the Pavin group as a differentiation trend dominated by crystal fractionation (Bourdier, 1980; Villemant et al., 2016). In this respect, the Pavin magmatic suite might be compared to the Chaîne des Puys series, the latter being compositionally more extensive since it shows silica-oversaturated trachytes. The Chaîne des Puys has been consistently modelled as resulting dominantly from crystal fractionation processes in crustal reservoirs (Maury et al., 1980; Villemant et al., 1981), in agreement with petrological and experimental constraints suggesting storage of the Chaîne des Puys trachytes at depths around 10 km (Martel et al., 2013). Recent geochemical modelling of the Pavin suite (Villemant et al., 2016) has stressed petrogenetic similarities between the Chaîne des Puys and Pavin suites, while pointing to some differences in the fractionation paths. The remoteness of the Pavin volcano from the differentiated volcanoes of the Chaîne des Puys and the small magma volumes involved (of the order of 30–40 Mm³ DRE for the Pavin magma) imply that the Pavin upper reservoir should be discrete and likely of small volume, so that some differences with the Chaîne des Puys differentiation processes are to be anticipated.

Table 1

Major-element composition and CIPW norms of the Pavin group and comparison with samples from the Chaîne des Puys.

	Pavin group			Chaîne des Puys				
	Pavin		Montchal	Montcineyre	Nugère	Clierzou		
Sample type	Fused pumice	Dense clast	Dense sample	Lava sample	Lava sample	Lava sample	Lava rock	Fused rock
Reference	This work	1	2	1	1	3	3	4
Major elements (wt %)								
SiO ₂	58.57	58.45	57.61	49.23	43.80	57.69	61.60	62.67
TiO ₂	1.38	1.30	1.37	2.35	2.80	1.13	0.85	0.75
Al ₂ O ₃	18.93	18.05	17.98	16.40	14.10	18.08	18.32	17.19
Fe ₂ O ₃	nd	nd	nd	nd	nd	6.90	4.80	nd
FeO	5.49	6.11	5.98	9.39	11.16	nd	nd	4.04
MnO	0.12	0.15	0.15	0.17	0.17	0.19	0.23	0.19
MgO	1.71	2.11	1.78	6.88	12.70	1.96	1.09	0.96
CaO	4.77	4.71	4.79	8.97	10.00	4.58	3.17	3.22
Na ₂ O	4.79	5.01	5.49	3.67	3.20	5.48	5.71	6.59
K ₂ O	3.82	4.11	4.49	1.97	1.45	3.44	3.91	4.09
P ₂ O ₅	0.40	nd	0.37	nd	nd	0.56	0.32	0.29
Diff. to 100	-1.29	-0.09	0.18	0.97	0.62	0.21	1.98	0.18
Na ₂ O/Na ₂ O + K ₂ O	0.56	0.55	0.55	0.65	0.85	0.61	0.59	0.62
P.I.	0.64	0.70	0.77	0.34	0.33	0.70	0.74	0.89
CIPW norm								
quartz	2.14	–	–	–	–	–	3.63	0.78
orthoclase	22.57	24.29	26.54	11.64	8.62	20.30	23.10	24.15
albite	40.54	42.39	40.96	22.40	3.51	46.34	48.31	55.77
anorthite	18.87	14.62	11.14	22.45	19.95	14.59	12.80	5.24
nepheline	–	–	2.98	4.69	12.86	–	–	–
apatite	0.99	–	0.92	–	–	1.39	0.80	0.73
ilmenite	2.62	2.47	2.60	4.46	5.35	2.15	1.61	1.43
magnetite	1.15	1.28	1.26	1.97	2.36	1.31	0.91	0.85
diopside	1.86	7.31	8.58	17.94	24.1	3.77	0.73	7.48
hypersthene	9.39	4.78	–	–	1.10	6.80	7.75	3.68
olivine	–	2.94	5.18	13.61	23.42	2.87	–	–

The fused sample of the Pavin trachyandesite was analysed by EMP (corrected for Na loss; Analytical methods given in Appendix A2), all other analyses are from the literature, with references as follows: (1) Bourdier, 1980; (2) Villemant et al., 2016; (3) Maury et al., 1980; (4) Martel et al., 2013 (corrected for Na loss). All analyses are recalculated to a total of 100 wt%, with 'Diff. to 100' giving the difference to the original total (negative for original sum > 100 wt%). P.I. is the peralkalinity index given as molar (Na₂O + K₂O)/Al₂O₃. nd for not determined.

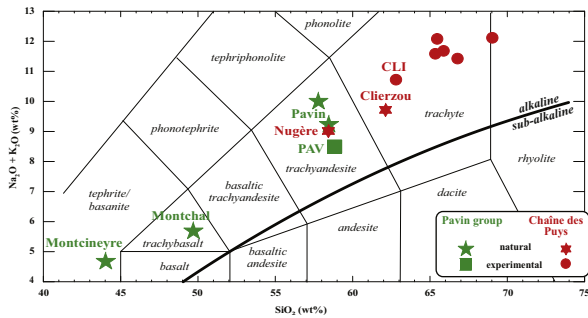


Fig. 2. Total alkalis versus SiO_2 bulk-rock compositions of the magmas from the Pavin group (in green) and the Chaîne des Puys (CDP; in red), as given in Table 1 (recalculated without P_2O_5 and total iron as FeO) and in Martel et al. (2013) for the CDP trachytes. Volcanic rock classification after Le Bas et al. (1986).

3. Results and discussion

3.1. Petrology of the Pavin trachyandesite

3.1.1. Lithology and whole-rock composition

The Pavin trachyandesite exhibits various textures, from dominantly pumice to denser and darker clasts that differ by vesicularity and groundmass microtexture, while their phenocryst assemblage and whole-rock composition do not show significant differences within the limits of our investigations. Major-element whole-rock compositions are given in Table 1 where the Pavin magma composition is compared to a closely analogous composition (Nugère trachyandesite) and a slightly more evolved one (Clierzou trachyte), both from the Chaîne des Puys volcanic field. All rocks show overall similarities, being metaluminous (P.I. in the 0.6–0.9 range) and close to silica saturation in the CIPW norm. The differentiation trend in the Chaîne des Puys has been thoroughly documented and is compositionally marked by a consistent decrease of FeO, MgO, CaO, and increase of alkalis with increasing SiO_2 (Camus, 1975; Martel et al., 2013; Maury et al., 1980). The Nugère (Chaîne des Puys) and Pavin trachyandesites have close contents for most major elements, though the Pavin composition is consistently richer in TiO_2 and K_2O , whereas poorer in P_2O_5 . In the Chaîne des Puys differentiation trend, the $\text{Na}_2\text{O}/\text{K}_2\text{O}$ ratio does not vary from the Nugère to the Clierzou compositions (Table 1) then it tends to decrease with increasing SiO_2 in the trachyte range, through an increase of K_2O at almost constant Na_2O (Martel et al., 2013 and references therein). The compositional differences between the Pavin and Nugère magmas, notably the K_2O -richer character of the Pavin magma, are sufficient to indicate that the Pavin magma belongs to a specific differentiation trend, i.e. distinct from the Chaîne des Puys one, as also evidenced by comparing trace-element compositions (Villemant et al., 2016)

3.1.2. Phenocryst assemblage and modal proportion

The phenocryst assemblage of the Pavin magma mostly consists of plagioclase, amphibole, clinopyroxene, and Fe–Ti oxides (Appendix B). Phenocrysts are found both isolated and as small glomeroporphyritic agglomerates. Apatite is a common accessory phase. Scarce biotite can be

found as inclusions in amphibole and isolated micro-phenocrysts. Modal proportions range from 10 to 23% (recalculated to 7 to 20 wt% crystallinity; Table 2). Such a variability of the phenocryst proportions could result from heterogeneous distribution at sample scale (e.g., due to the tendency of phenocrysts to agglomerate) or might be acquired through crystallization along the course of the eruption. No attempt has been made in this study to evaluate the variability of magma crystallinity through the Pavin deposit stratigraphy

To some extent, the phenocryst assemblage of the Pavin trachyandesite can be compared qualitatively to counterparts from the Chaîne des Puys. Although compositionally close to the Pavin sample, the Nugère trachyandesite is almost aphyric. Other trachyandesites in the Chaîne des Puys, although scarce and volumetrically trivial, typically contain as Fe–Mg phenocrysts, both amphibole (more or less stable) and stable clinopyroxene, and lack biotite (Maury et al., 1980). Further, the couple clinopyroxene–amphibole is still present in the less differentiated trachytes, Aumone and Clierzou, which also lack biotite (Boivin et al., 2015). In contrast, biotite is a systematic phase in the more differentiated trachytes, either as the single Fe–Mg phase or accompanied by either amphibole or clinopyroxene, not both (Boivin et al., 2015; Martel et al., 2013). The Pavin phenocryst assemblage thus compares well with the Chaîne des Puys magmas at comparable levels of differentiation. The rare occurrence of biotite in the Pavin magma, at lower SiO_2 than needed for biotite appearance in the Chaîne des Puys series, might reflect the higher amount of K_2O in the Pavin magma compared to the Chaîne des Puys ones to a similar differentiation degree.

3.1.3. Mineralogy

The natural phases were analysed following the method given in Appendix A2 and the compositions given in Appendix C

Plagioclase, although frequently fractured, is euhedral with clear rims, and variously zoned with frequent cloudy to sieved core textures. The plagioclase composition spreads from 32 to 58 mol% of anorthite (An32 to An58), with an orthoclase content not exceeding 5% (<Or5) and consistently increasing as An decreases, (Fig. 3a).

Table 2

Modal proportions of the Pavin pyroclasts.

Reference ^a	This study		1		2			
	pumice		pumice		pumice		all	
Lithology ^b	pumice		pumice		pumice		all	
Proportion ^c	%	wt%	%	wt%	%	wt%	%	wt%
Plagioclase	14	13	5	4	6.5	6	6	6
Amphibole	4	3	3	2	2	1	7	6
Clinopyroxene	1	2	1	1	1.5	1	7	5
Fe–Ti oxides	4	2	1	<1	0.5	<1	3	1
Crystallinity ^d	23	20	10	7	10.5	8	23	18

^a From (1) Bourdier (1980) and (2) Leyrit et al. (2016).

^b pumice for pumice clasts and all denotes analyses on 17 thin sections encompassing pumice to dense clasts (mean mineral content).

^c % gives the void-free modal proportion determined from point counting using an optical microscope and wt% is mass proportion recalculated with the respective mineral densities as defined in Appendix A2.

^d Including apatite (<0.5) and scarce biotite.

Plagioclase rims have a restricted compositional range of An_{35–38}, while most of the cores have compositions of An_{45–62}, with the exception of one profile showing a reverse zoning with core composition down to An₃₂. From core to rim, the plagioclases show either smooth An decrease or drastic drops (Fig. 3b). In the Chaîne des Puys, for comparison, plagioclases in the trachyandesites are

reported as being mostly in the range of andesine (An_{30–50}; Maury et al., 1980). The plagioclases of the less differentiated Chaîne des Puys trachytes are also andesine, in the range An_{30–42}, with a mean composition of An₃₈ (Boivin et al., 2015; Martel et al., 2013).

Amphibole occurs as 1–2-mm-long, euhedral and unresorbed phenocrysts with common inclusions of

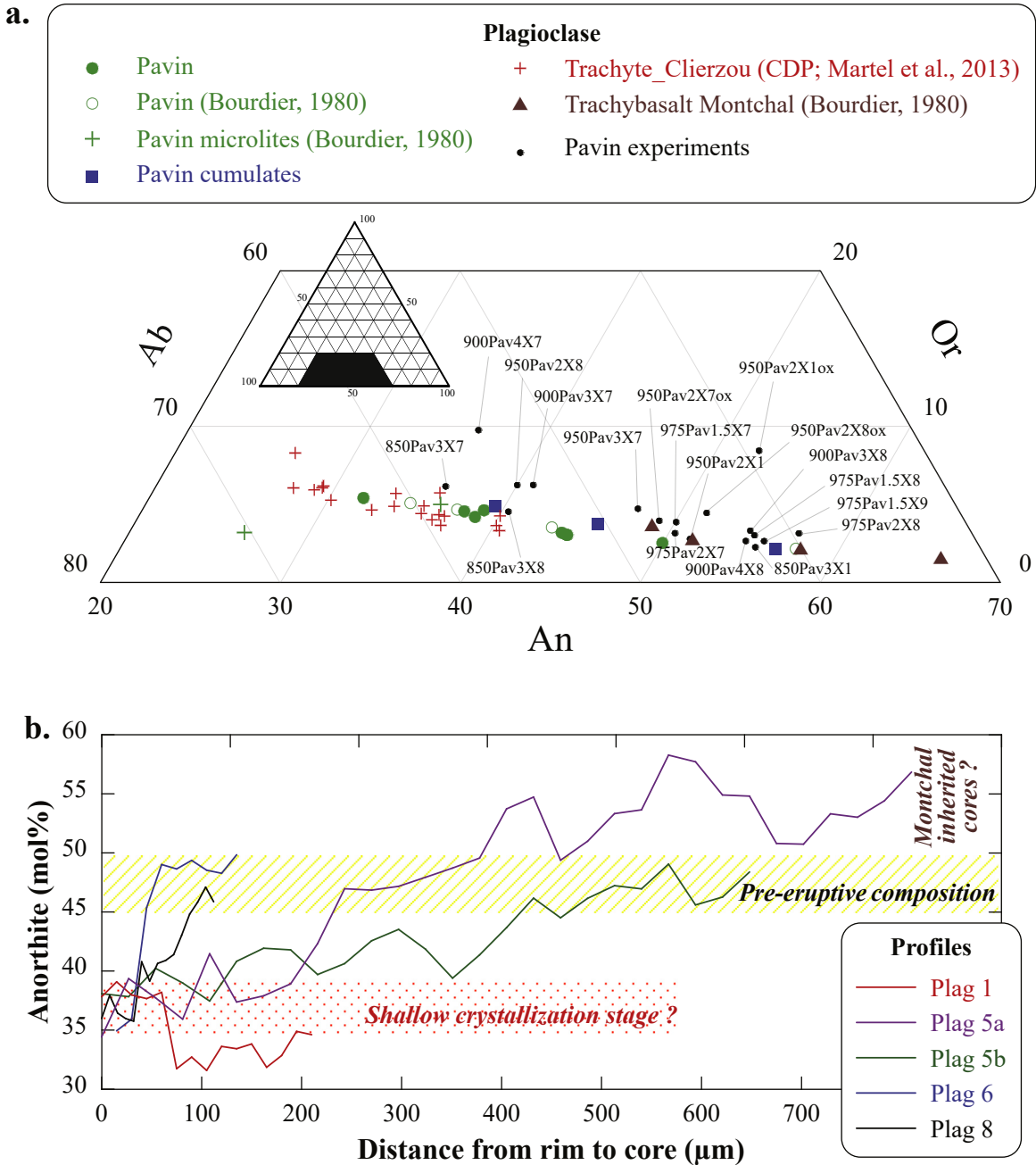


Fig. 3. (a) Natural and experimental plagioclase compositions recalculated as anorthite (An), albite (Ab), and orthoclase (Or) mol%, as given in Appendix C1 and (b). (b) Analytical profiles from rim to core, with the yellow box showing the An_{45–50} plateau value present in nearly all plagioclases and interpreted as the pre-eruptive compositions in the reservoir (see text). Higher An content may be inherited cores from the Montchal trachybasalt (as suggested by the Montchal plagioclase composition in a). The red box shows the An_{35–40} rim composition present in all phenocrysts that may reflect a shallow level of crystallization (see text).

oxides, apatite and biotite (Appendix B2). The amphiboles are kaersutites and hastingsites after Leake et al. (1997), showing a rather scattered range in contents of SiO₂ (38.5–40.7 wt%), Al₂O₃ (11.1–13.9 wt%), Al^{IV} (1.9–2.2), TiO₂ (4.1–5.3 wt%), and Mg# (0.61–0.66) (Appendix C2). Amphibole-rich cumulates are common in the Pavin deposit, notably in the upper part of the deposit stratigraphy. The amphibole from the cumulates is mostly kaersutite that plots separately from the amphiboles analysed in the juvenile pyroclasts (Fig. 4). This is good evidence that the latter form a truly phenocrystic population, without any contribution of xenocrysts of cumulative origin. Within the phenocrystic amphibole population, core and rim compositions do not show systematic variations and are close to each other in the limits of our data set. Thus, the compositional scattering of the amphibole phenocrysts is not related to any significant zoning and likely reflects variations in the crystallization conditions (liquid composition and/or intensive parameters) within the magma reservoir. Amphiboles from the low-silica Clierzou trachyte are also compositionally scattered, but commonly show slightly lower contents in A-site cation number, Al^{IV} content, and Mg# (Fig. 4).

The clinopyroxenes in the juvenile pyroclasts are 1–2 mm long, have smoothed more or less resorbed rims, and contain frequent glass inclusions. They are salites with 44–48 mol% wollastonite (Wo44–48) and 34–45 mol% enstatite (En34–45) (Fig. 5a), with notable scattering in SiO₂ and Al₂O₃ contents (Fig. 5b; Appendix C3). By comparison, clinopyroxenes from cumulates are mostly less calcic (Wo41–47) and more magnesian (En39–46), and are on average poorer in SiO₂ and richer in Al₂O₃ and TiO₂ (Fig. 5b; Appendix C3). The compositions of the clinopyroxenes from the cumulates are even more scattered than those of the trachyandesite, suggesting large variations in the crystallization conditions. Compared to the Pavin

pumice, clinopyroxenes from the Clierzou trachyte are mostly less calcic (Wo41–47) and more magnesian (En39–46; Fig. 5a), and are on average poorer in SiO₂ and richer in Al₂O₃ (Fig. 5b).

Biotite is scarce and contains about 6 wt% TiO₂, 14.5 wt% MgO and 13–14 wt% Al₂O₃, less than 0.4 wt% MnO and F, with Mg# ~0.65 (Fig. 6; Appendix C4). Comparatively, the Clierzou trachyte does not contain biotite. Biotites are only present in the most differentiated trachytes (>65 SiO₂ wt%), in which they are poorer in magnesium compounds (e.g., Mg# ~0.55; Fig. 6) and slightly richer in alumina (14–15 wt% Al₂O₃ in the Vasset trachyte; Martel et al., 2013) than the Pavin biotites.

Fe–Ti oxides are both magnetite–ulvöspinel and ilmenite–hematite solid solutions (Appendix C5). The isolated phenocrysts often show strong textures of exsolution, whereas Fe–Ti oxides found as mineral inclusions in mostly clinopyroxene and amphibole are texturally and compositionally homogeneous. Fe–Ti oxides in amphibole and clinopyroxene do not show systematic compositional differences. Apparently, homogeneous isolated phenocrysts show compositions similar to those found as inclusions, i.e. titanomagnetite with 67–78 mol% magnetite (Mt67–78; with 0.8–1.3 wt% MnO, 79–83 wt% FeO, and 7.5–11.5 wt% TiO₂) and ilmenite with 63–68 mol% ilmenite (Ilm63–68; with 0.8–1 wt% MnO, 55–57 wt% FeO, and 36–38 wt% TiO₂). For comparison, the magnetites and ilmenites from the Clierzou trachytes are Mt- and Ilm- richer, respectively (Mt80–90 and Ilm70–90; Martel et al., 2013).

Glass inclusions are frequently trapped in plagioclases and clinopyroxenes, but are mostly devitrified in the former whereas mostly glassy in the latter, so that all analysed glass inclusions were clinopyroxene-hosted, with one in a magnetite. The compositions are trachytic, showing narrow ranges of 64–66 wt% SiO₂ and 11.5–12.5 wt% alkalis

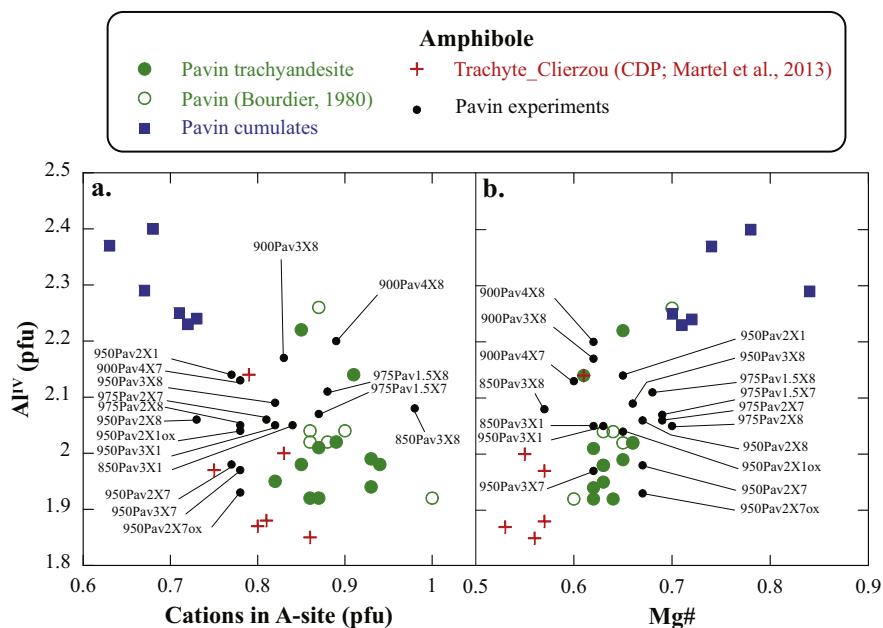


Fig. 4. Natural and experimental amphibole compositions recalculated as Al^{IV} content versus (a) cations in A-site (pfu) and (b) Mg#, as given in Appendix C2.

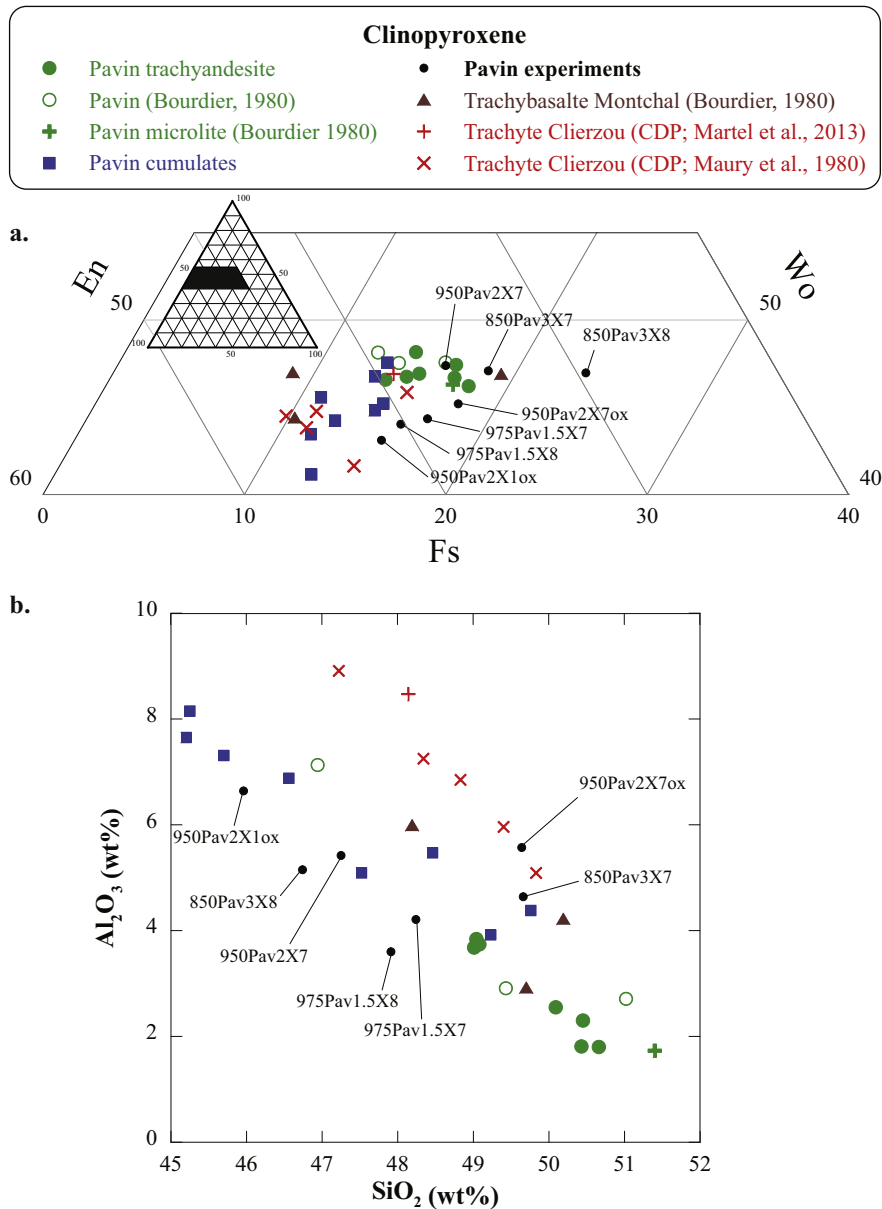


Fig. 5. Natural and experimental clinopyroxene compositions recalculated as (a) enstatite (En), wollastonite (Wo), ferrosilite (Fs) mol% and (b) Al_2O_3 versus SiO_2 wt%, as given in [Appendix C3](#).

([Appendix C6](#)). The microlite-poor matrix glasses of the Pavin pumices have compositions similar to those of the glass inclusions ([Fig. 7](#)). The Pavin glasses overall broadly compare with the bulk-rock compositions of the intermediate-silica trachytes of the Chaîne des Puys (Kilian, Vasset, Sarcouy, Puy de Dôme), except for lower Na_2O and higher K_2O contents (both by ~ 1 wt%; [Fig. 7](#)). The K_2O -richer character of the Pavin whole-rock trachyandesite compared to Chaîne des Puys analogues.

The H_2O contents of the Pavin glasses are inferred from a calibrated by-difference method (see [Appendix](#)

[A2](#)), which assumes that volatiles other than H_2O can be neglected. Fluorine contents are below 0.5 wt% in the Pavin glass inclusions ([Appendix C6](#)), in agreement with the fluorine, chlorine, and sulphur contents below 0.5 wt% for the glass inclusions of the Chaîne des Puys trachytes ([Martel et al., 2013](#)). We thus assume that H_2O is by far the most abundant volatile species and that the inferred values cannot be overestimated by more than 0.5 wt%. The range of H_2O content is large, with the matrix glasses showing low contents (<1.5 wt%) and the glass inclusions ranging between 1.1 and 5.3 wt% H_2O ([Fig. 8](#); [Appendix C6](#)).

3.2. Crystallization conditions retrieved from the natural samples

3.2.1. Phase assemblage and compositions relevant to the reservoir conditions

The natural pumice pyroclasts contain phenocrysts of plagioclase, amphibole, clinopyroxene, magnetite, ilmenite, and minor apatite. The scarcity of biotite, only found as inclusions in amphibole or rare isolated microphenocrysts, likely reflects inherited crystals.

We selected pumice clasts from an explosive event during which magma was supposed to ascend rapidly from the storage region to the surface. This has the advantage to minimize syn-eruptive crystallization, although the samples do contain some microlites that evidence crystallization after reservoir exit. If such syn-eruptive crystallization is negligible, the pre-eruptive phase compositions are provided by the phenocryst rims in equilibrium with the interstitial glass (or alternatively glass inclusions if they were not compositionally modified after entrapment). The plagioclase phenocrysts show rim compositions of An35–40 (Fig. 3b) that turned out to be impossible to reproduce under realistic storage conditions, as evidenced experimentally below. Rather, the plateau range of An46–52 present in most of the plagioclase phenocrysts seems to represent the pre-eruptive compositions, whereas compositions <An40 may reflect crystallization stages at shallower levels. Contrary to plagioclase, the other phenocrysts do not show significant compositional zonings, possibly reflecting their slower crystallization kinetics or lower compositional sensitivity to (lower) pressure and melt H₂O content. The residual glasses of the erupted products may have been compositionally modified by syn-eruptive crystallization during magma ascent in the volcanic conduit (e.g. phenocryst rims and microlites). In contrast, melt trapped as inclusions by phenocrysts growing in the reservoir may be more representative of the pre-eruptive melt composition. Yet, microlite-bearing residual glasses and glass inclusions globally cover the same compositional range (Fig. 7), suggesting a similar compositional evolution. In particular, the Fe–Mg partition coefficients between glass inclusion and host clinopyroxene give a mean value of 0.11 ± 0.03 , whereas reaching 0.25 ± 0.04 for the experimental melt–clinopyroxene pairs (in agreement with the value of 0.28 ± 0.09 given by Putirka, 2008), which likely suggests some compositional modification of the melt inclusions after entrapment.

Therefore, the experiments should reproduce 7–20 wt% phenocrysts consisting of An49 ± 3 plagioclase, amphibole with 12 ± 1 wt% Al₂O₃ (Am12 ± 1), Wo46 ± 2 clinopyroxene, Mt72 ± 5 magnetite, Ilm65 ± 2 ilmenite, and apatite in a glass with less than 65 ± 1 wt% SiO₂ and up to 5.5 wt% H₂O, as shown by the glass inclusions (keeping in mind though that they were mostly modified after entrapment).

3.2.2. Intensive parameters inferred from the natural assemblage

Pairs of coexisting Mt and Ilm, either trapped in phenocrysts (clinopyroxene or amphibole) or as individual phenocrysts, can be used to constrain the temperature (T) and oxygen fugacity (f_{O_2}) prevailing at the time of their

crystallization, provided they co-crystallized from the same parental melt. Pairs that were positively tested for chemical equilibrium (after Bacon and Hirschmann, 1988) were used to calculate T – f_{O_2} values following the formulation of Sauerzapf et al. (2008). Since this formulation is not calibrated originally for trachyandesitic to trachytic compositions, we tested it against the experimental oxides that crystallized under controlled T and f_{O_2} . The results give T estimates up to 40 °C and f_{O_2} up to 1.3 log units, but mostly agree within 0.3 log units with the experimental conditions (Appendix D1), so that we validated the method for the Pavin compositions. The calculations on the natural Mt–Ilm pairs give T between 850 and 970 °C and f_{O_2} in the range from NNO+1.3 to +1.9.

No thermodynamic model is adequately calibrated to estimate total pressure (P) for trachyandesite compositions and phase assemblages such as the Pavin ones. Nevertheless, the formulations of Ridolfi and Renzulli (2012), based on amphibole composition, were tested. Compared to the run P , the calculations give significant and systematic P overestimations by over 100 MPa (e.g., 105 to 304 ± 50 MPa; Appendix D2). Such calculations also overestimate T by 41–146 °C, whereas underestimating f_{O_2} by about 1 log unit (Appendix D2). Therefore, we cannot consider the formulations of Ridolfi and Renzulli (2012) relevant for amphiboles crystallizing from the Pavin trachyandesite.

The pre-eruptive H₂O content may be inferred from H₂O dissolved in glass inclusions, assuming volatile tightness after reservoir exit. Although the large variability in H₂O contents (1.1–5.3 wt%; Fig. 8) likely suggests that not all glass inclusions remained sealed after reservoir exit, the H₂O-rich ones suggest entrapment pressures of

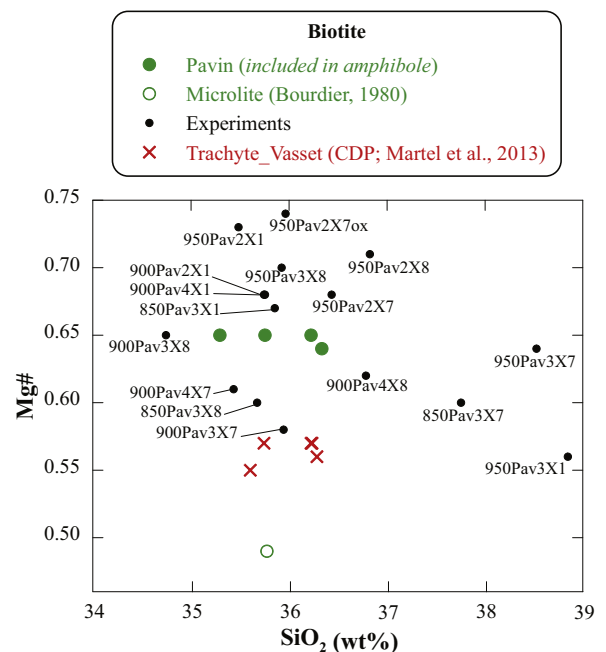


Fig. 6. Natural and experimental biotite compositions recalculated as Mg# versus SiO₂ wt%, as given in Appendix C4.

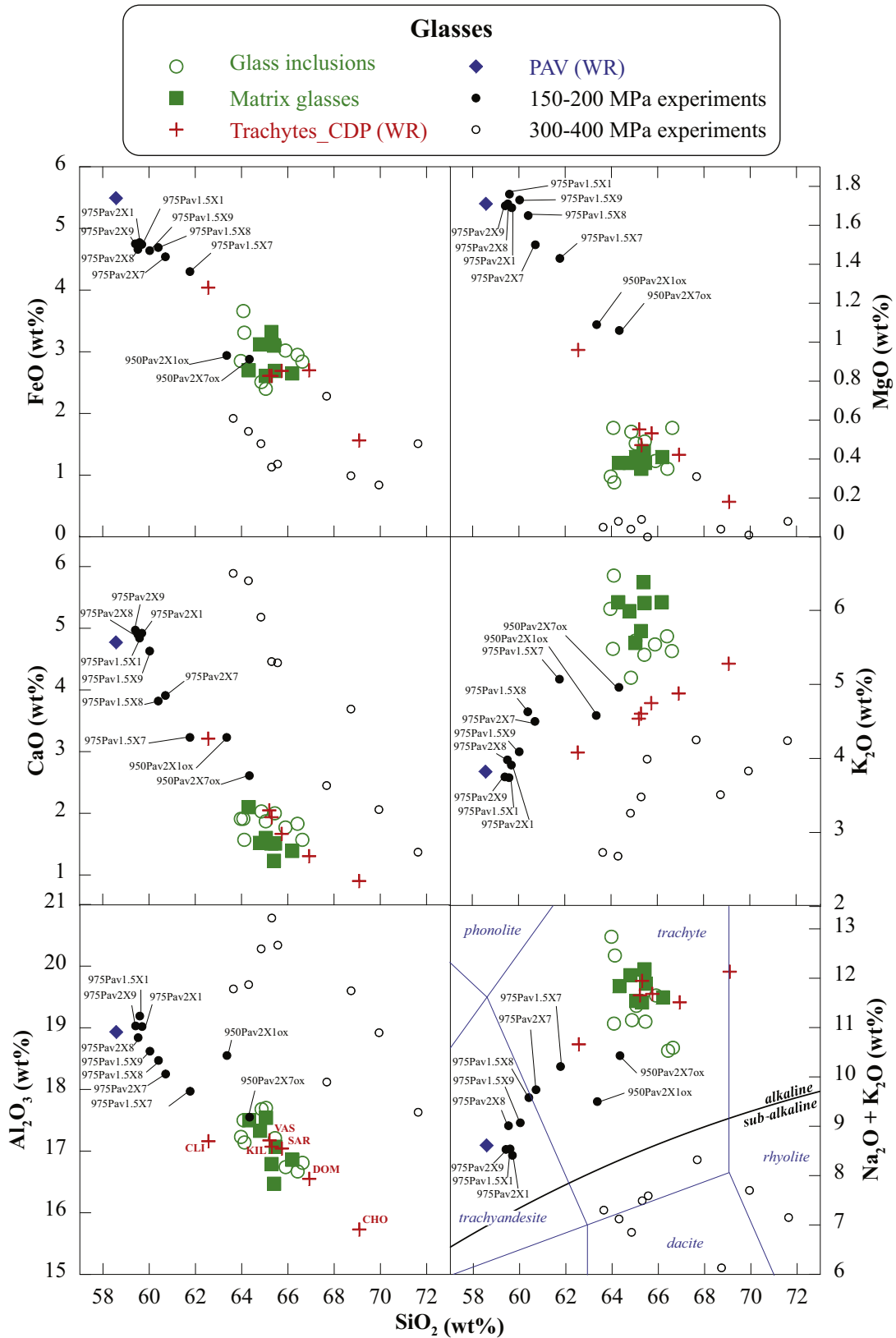


Fig. 7. Natural and experimental glass compositions plotted in Harker diagrams, as given in Appendix C6 (glasses are corrected for Na₂O and normalized to 100 wt% on a volatile-free basis).

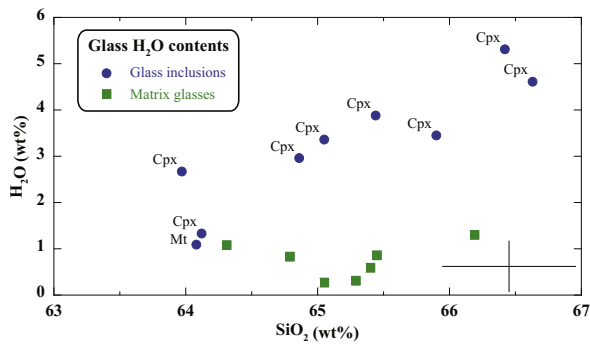


Fig. 8. Melt H₂O content of glass inclusions (circles; clinopyroxene- or magnetite-hosted) and matrix glasses (squares) as given in Appendix C6.

~120 MPa (Di Matteo et al., 2004; minimum value if not H₂O saturated).

3.3. Experimentally-determined storage conditions of the Pavin trachyandesite

In order to better constrain the storage conditions, phase-equilibrium experiments starting from the fused Pavin trachyandesite were performed following the method given in Appendix A1. The experimental conditions were chosen to cover the range of intensive parameters inferred from the natural assemblage. Therefore, crystallization experiments were performed from 850 to 950 °C, 150–400 MPa, NNO+2, and X_{H_2O} in ranging from 0.7 to 1 (i.e. melt H₂O contents from 4.5 to 9.5 wt%; Table 3). Below, we compare the natural phase assemblage, proportion, and compositions to those obtained experimentally (Fig. 9, with phase relationships and compositions described in Appendix E).

At ~400 MPa and NNO+1.5, stable plagioclase, amphibole, and clinopyroxene require H₂O contents around 8 wt% and T close to 900 °C (Fig. 9c). Yet, the crystallinities of the run products at these conditions are much higher (~70 wt%) than those of the Pavin samples (11–20 wt%), biotite is ubiquitous although not considered as stable in the reservoir, and the experimental glass compositions are systematically off the trend defined by the Pavin whole-rock and natural glasses in CaO, Al₂O₃, and alkali contents (Fig. 7). Varying T from 850 to 1000 °C would not help reconciling these discrepancies, since biotite would still be present, amphibole and clinopyroxene would not coexist, and/or the modal proportions would be too low (Fig. 9). Therefore, 400 MPa is not a realistic P for storing the Pavin magma.

Similarly, at ~300 MPa and NNO+1, plagioclase, amphibole, and clinopyroxene are stable at T -H₂O conditions for which crystallinities are ≥40 wt%, biotite is present (Fig. 9b), and the residual glasses hardly agree with the trend defined by the Pavin whole-rock and natural glasses (Fig. 7). Therefore, it rules out 300 MPa as a possible storage P for the Pavin reservoir.

At 150–200 MPa, ~NNO+1, and 950–975 °C, H₂O saturation conditions (7.0 wt% H₂O) do not allow clinopyroxene crystallization. Even if slightly more oxidized conditions could compensate for this, the plagioclase An content

would be significantly higher than An52 (Fig. 9a). Similarly, for lower H₂O contents of ~6 wt%, the plagioclase An content is between 51 and 57 wt% (Fig. 9b). For H₂O contents between 4.5 and 5.5 wt%, however, ~An50 crystallizes, together with Wo44–47 and Am11–12 (Fig. 9c). The Fe–Ti oxide compositions, Mt60–61 and Ilm84–87, likely suggest too low f_{O_2} conditions compared to the natural Fe–Ti oxides (Mt72 ± 5 and Ilm65 ± 2). In view of the Mt84 that crystallized together with hematite at NNO+2, it is reasonable to predict that a f_{O_2} intermediate between NNO+1 and +2 would allow Fe–Ti oxide compositions close to the natural ones. This is in agreement with the natural Mt–Ilm pairs suggesting NNO+1.3 to +1.9 for T between 850 and 970 °C. The 15–22 wt% crystallinity at 975 °C for H₂O contents of 4.5–5.5 wt% is compatible with the natural crystallinities (7–20 wt%), but the residual liquid contains ~62 wt% SiO₂, i.e. significantly less than for the natural glasses (64–66 wt% SiO₂). Vice versa, experimental liquids with 64 wt% SiO₂ result from crystallinities much higher than expected from the natural samples (e.g., 76 wt% crystals, including 36 wt% plagioclase, at 950 °C, ~5.5 wt% H₂O, and NNO+2). Yet, the natural residual liquids crystallized and differentiated during ascent in the conduit, thus not excluding liquids with 62 wt% SiO₂ as possible pre-eruption compositions.

In summary, the storage conditions for the Pavin trachyandesite could be close to 150–200 MPa (~5.5–7.0 km in depth), 950–975 °C, NNO+1.5, and melt H₂O content about 4.5–5.5 wt% (Fig. 10). Noteworthy, these P - T conditions are outside, but close to the stability field of biotite, and inside, but close to clinopyroxene destabilization, which may in both cases account for their presence but low abundance in the natural samples.

3.4. Reservoir and eruption dynamics

The Pavin juvenile products provide petrological information on (1) the reservoir dynamics prior to eruption, and (2) the eruptive conditions upon ascent of the magma towards surface.

3.4.1. Reservoir dynamics

The juvenile pumice shows a great variability in many petrological features as shown above, notably phenocryst proportions, amphibole and clinopyroxene compositional scatter, and plagioclase zonings. Such heterogeneities likely point to variability in the differentiation process, in terms of liquid/crystal ratio and intensive parameters. This is further demonstrated by the inability of any of our phase-equilibrium experiments to fulfil the observed natural assemblage and phase compositions. Actually, the inferred intensive parameters can only be bracketed, the somewhat limited range of parameters fixed above representing the conditions for the mean assemblage and compositions. Indeed, the delimited P - T field for the Pavin storage conditions is tightly bordered by the clinopyroxene, ilmenite, and biotite appearance curves, so that slight P - T - f_{O_2} variations may drastically modify the phase assemblage and the liquid/crystal ratio (e.g., decreasing T to 950 °C leads to biotite crystallization and total crystallinities of ~70 wt%; Fig. 9c)

Table 3
Experimental conditions, phase assemblages and proportions.

Sample #	X_{H_2O} in	H_2O_{melt} (wt%) ^a	Major phases (proportion in wt%)	χ (wt%) ^b	χ_{SiO_2} (wt%) ^c
Run 1, 300 MPa, 900°C, NNO+0.8 (sensors), 4 days					
900Pav3X1	1.00	8.5	Gl ₍₈₄₎ + Am ₍₃₎ + Bt ₍₉₎ + Mt ₍₄₎ + Ilm _(0.2) + Ap	17	36.7
900Pav3X8	~0.9	8.0	Gl ₍₇₈₎ + Am ₍₈₎ + Bt ₍₅₎ + Pl ₍₅₎ + Mt ₍₄₎ + Ilm _(0.1)	22	41.7
900Pav3X7	0.75	7.4	Gl + Am + Bt + Pl + Mt + Ilm	~70	
Run 2, 294 MPa, 950°C, ~NNO+0.5 (from Fe–Ti oxide thermo-oxymetry), 5 days					
950Pav3X1	1.00	8.5	Gl ₍₈₃₎ + Am _(<1) + Bt ₍₁₅₎ + Mt ₍₂₎	16	38.8
950Pav3X8	0.84	7.7	Gl ₍₇₇₎ + Am ₍₃₎ + Bt ₍₁₄₎ + Mt ₍₅₎ + Ilm ₍₁₎	23	36.6
950Pav3X7	0.69	7.0	Gl + Am + Bt + Pl + Mt + Ilm	~70	
Run 3, 284 MPa, 850°C, NNO+0.8 (sensors), 5 days					
850Pav3X1	1.00	8.5	Gl ₍₆₅₎ + Am ₍₅₎ + Bt ₍₉₎ + Pl ₍₁₇₎ + Mt ₍₃₎ + Ilm ₍₁₎	35	45.6
850Pav3X8	0.83	7.5	Gl ₍₆₀₎ + Am ₍₁₄₎ + Bt ₍₃₎ + Pl ₍₂₄₎ + Cpx ₍₇₎ + Mt ₍₂₎ + Ilm _(0.3)	40	48.3
850Pav3X7	0.67	6.7	Gl ₍₆₀₎ + Bt ₍₁₁₎ + Pl ₍₄₅₎ + Cpx ₍₄₎ + Mt ₍₃₎ + Ilm _(0.6)	63	53.8
Run 4, 192 MPa, 950°C, NNO+2.1 (sensors), 8 days					
950Pav2X1ox	1.00	6.9	Gl ₍₇₆₎ + Am ₍₅₎ + Pl ₍₁₅₎ + Cpx _(0.5) + Mt ₍₂₎ + Hem ₍₂₎	24	50.2
950Pav2X7ox	~0.75	5.7	Gl ₍₂₄₎ + Am ₍₁₅₎ + Bt ₍₁₀₎ + Pl ₍₃₆₎ + Cpx ₍₁₁₎ + Mt ₍₃₎ + Hem ₍₁₎	76	49.9
Run 5, 365 MPa, 900°C, ~NNO+1.5 (from Fe–Ti oxide thermo-oxymetry), 4.5 days					
900Pav4X1	1.00	9.5	Gl ₍₈₄₎ + Am ₍₄₎ + Bt ₍₇₎ + Mt ₍₄₎ + Ilm _(<1) + Ap ₍₁₎	16	36.5
900Pav4X8	0.80	8.3	Gl ₍₆₀₎ + Am ₍₁₁₎ + Bt ₍₆₎ + Pl ₍₂₀₎ + Mt ₍₃₎ + Ilm ₍₁₎	40	45.9
900Pav4X7	~0.70	7.8	Gl + Am/Cpx + Bt + Pl + Mt + Ilm	~70	
Run 6, 214 MPa, 950°C, NNO+0.7 (sensors), ~2 days (failed)					
950Pav2X1	1.00	6.9	Gl + Am + Bt + Pl + Mt + Ilm	-	
950Pav2X8	0.76	6.3	Gl + Am + Bt + Pl + Mt + Ilm + Ap	-	
950Pav2X7	0.67	5.8	Gl + Am + Bt + Pl + Cpx + Mt + Ilm	-	
Run 7, 192 MPa, 975°C, ~NNO+1 (no sensors), 7.5 days					
975Pav2X1	1.00	6.9	Gl ₍₉₉₎ + Mt ₍₁₎	1	
975Pav2X9	0.90	6.6	Gl ₍₉₉₎ + Mt ₍₁₎	1	
975Pav2X8	0.77	6.3	Gl ₍₉₆₎ + Am ₍₁₎ + Pl ₍₂₎ + Mt ₍₁₎	4	47.9
975Pav2X7	0.68	5.8	Gl ₍₈₅₎ + Am ₍₂₎ + Pl ₍₁₁₎ + Mt ₍₂₎	15	51.5
Run 8, 148 MPa, 975°C, ~NNO+1 (no sensors), 4 days					
975Pav1.5X1	1.00	5.8	Gl ₍₉₉₎ + Mt ₍₁₎	1	
975Pav1.5X9	0.89	5.4	Gl ₍₉₃₎ + Pl ₍₅₎ + Mt ₍₂₎	7	51.7
975Pav1.5X8	0.77	5.0	Gl ₍₈₇₎ + Am ₍₁₎ + Pl ₍₉₎ + Cpx ₍₂₎ + Mt ₍₁₎	13	50.0
975Pav1.5X7	0.69	4.5	Gl ₍₇₈₎ + Am ₍₁₎ + Pl ₍₁₇₎ + Cpx ₍₂₎ + Mt ₍₂₎	22	52.1

^a Melt H₂O content calculated after Eq. (1) in Appendix A2.

^b Crystallinity calculated by mass balance, as defined in Appendix A2.

^c Crystal SiO₂ content in wt% calculated as the sum of the mass fractions of each mineral (i.e. Am, Bt, Pl, Cpx; from the 'Major phase' column, divided by the total fraction) by each mineral SiO₂ contents (as given in Appendix C1–4).

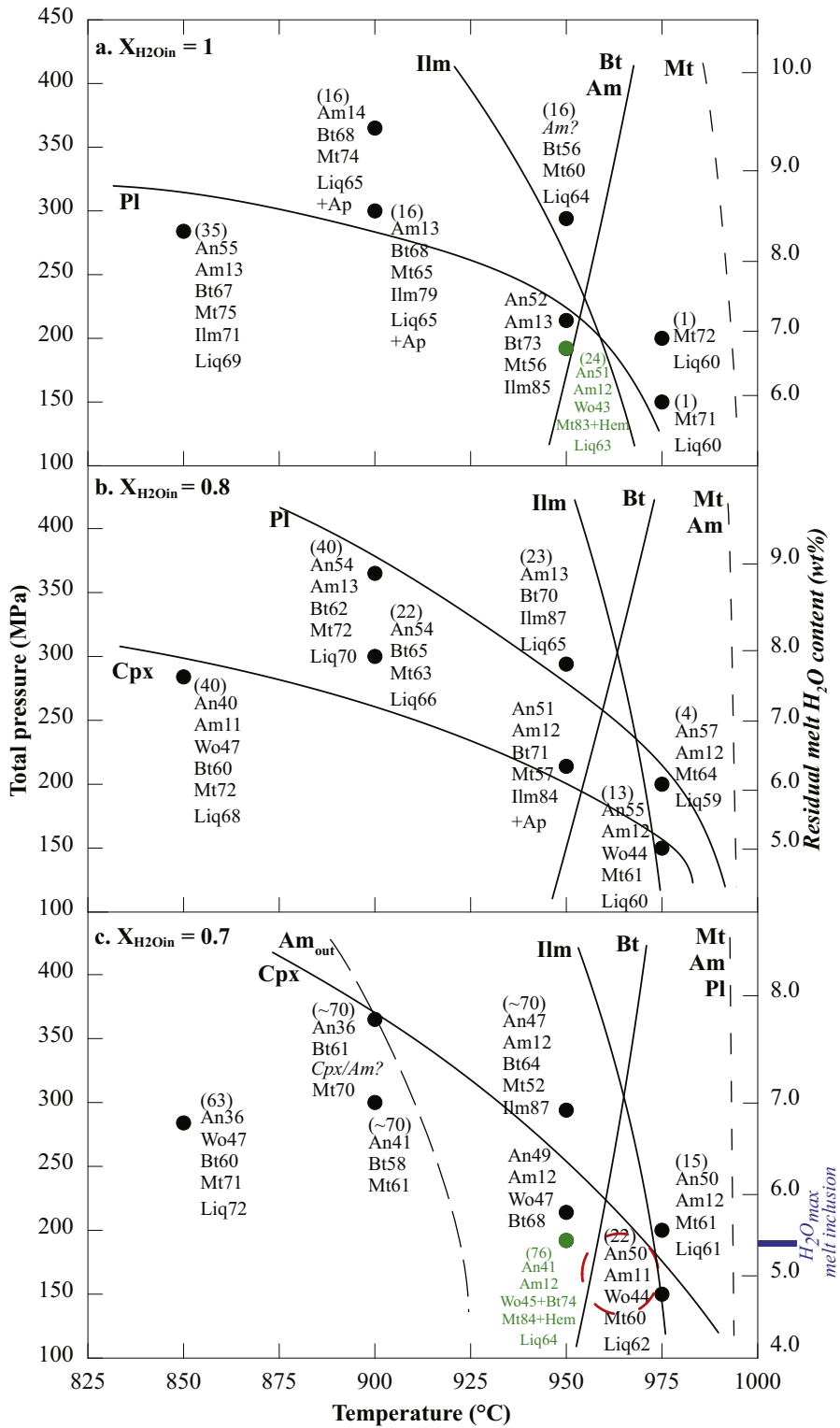
The Pavin volcano is an isolated monogenetic crater of trachyandesitic composition, suggesting that it is fed by a short-lived reservoir of likely small volume. Small polycrystalline cumulates and free cumulative crystals are abundant in the uppermost part ash fraction of the pyroclastic sequence, suggesting that the eruption tapped lower cumulative parts of the reservoir. This highlights that the reservoir was likely emptied and thus of small volume. We argue that the observed variability in phase compositions is well explainable if considering a small volume reservoir where magma evolves under strong gradients of physical parameters (notably temperature that in turn controls phase assemblage and magma crystallinity). In this respect, the Pavin case contrasts with many documented large volume silicic eruptions, notably ignimbritic ones, where phase assemblage and compositions are more homogeneous, likely resulting from the buffering effect of large magma volume on the controlling physicochemical parameters.

3.4.2. Conduit dynamics

The incompatibility between the plagioclase rim compositions of An_{32–40} (Fig. 3b) and the experimental

compositions in the 150–400 pressure range (Fig. 9) argues for plagioclase crystallization upper in the conduit. Some of the plagioclase rims show a gradual An decrease, whereas others show a drastic drop (Fig. 3b), suggesting that the magma may have reached this intermediate storage level following different ascent rates. Similarly, some clinopyroxene-hosted melt inclusions preserved the pre-eruptive melt H₂O contents of ~4.5–5.5 wt%, whereas most of them are poorer in H₂O (Fig. 8), likely reflecting imperfect tightness and connection with the residual liquid during magma ascent (Humphreys et al., 2008). Most of the glass inclusions contain ~3 wt% H₂O, suggesting quench pressures around 50 MPa (Di Matteo et al., 2004). Such a melt inclusion re-equilibration pressure is compatible with crystallization of An_{32–40} plagioclase. Therefore, we assume that parts of the magma crystallized at an intermediate level of ~50 MPa (i.e. 2.0 km depth), whereas other batches ascended fast enough to preserve the pre-eruptive phase compositions and H₂O contents. The 0.3 to 1.2 wt% H₂O of the residual glasses mark a later degassing that is not associated with crystallization, probably due to the slow kinetics and large crystal nucleation delays prevailing at low pressures (Mollard et al., 2012). The residual glass

Pavin trachyandesite (7-20 wt% phenocrysts)
 $An_{49}_{+3} Am_{12}_{+1} Wo_{46}_{+2} Mt_{72}_{+5} Ilm_{65}_{+2} Liq_{<65}_{+1}$



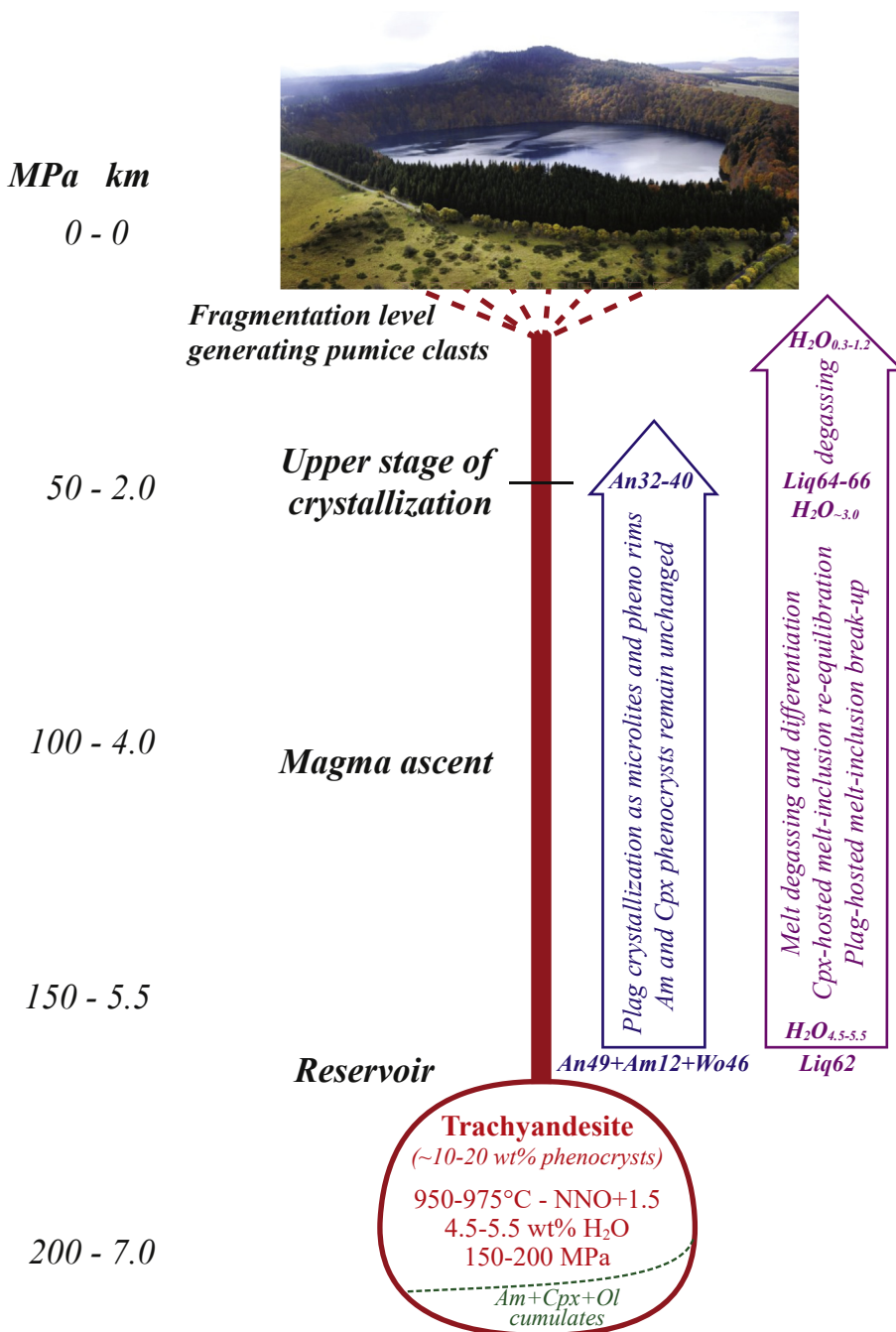


Fig. 10. Schematic view of the plumbing system beneath the Pavin volcano, showing the magma storage conditions and the eruptive scenario based on petrological information. Phase abbreviations and composition as in Fig. 9. See text for explanations.

Fig. 9. Pressure–temperature phase stability of the Pavin trachyandesite as a function of H₂O content. (a) X_{H₂O} in = 1 (H₂O saturation), (b) X_{H₂O} in = 0.8, and (c) X_{H₂O} in = 0.7 (black and green circles for NNO+1 and NNO+2, respectively). The right Y-axes give melt H₂O content calculated after Eq. (1) in Appendix A2. The point labels give the crystallinity in wt% (in bracket) followed by the phase compositions: plagioclase as anorthite mol% (An), amphibole (Am) as Al₂O₃ wt%, clinopyroxene as wollastonite mol% (Wo), biotite as Mg#, titanomagnetite as magnetite mol% (Mt), and glass as liquid (Liq) SiO₂ wt% (all compositions are given in Appendix C). The crystallinity (void-free basis) and phase compositions of the natural pumice samples are given in figure title. The dashed red circle shows the experimental conditions that best reproduce the natural phase assemblage and compositions.

H₂O contents below 1.2 wt% reflect pumice clast quenching at fragmentation depth below 1 km ($P \leq 20$ MPa; Fig. 10)

3.5. Differentiation trend and comparison with the volcanic suite of the Chaîne des Puys

Plotted in Harker diagrams, the experimental residual glasses show major compositional differences with pressure, i.e. the 150–200 MPa glasses are trachyandesitic to trachytic (alkaline trend), whereas the 300–400 MPa glasses are dacitic to rhyolitic in terms of silica and alkali contents (sub-alkaline trend; Fig. 7). In details, the compositional differences in the residual glasses from both pressure series come from major differences in the crystallized mineral assemblage and proportion, as demonstrated for basalts in the pioneer work by Grove and Baker (1984). This is highlighted by the total silica content of the crystallized minerals, which is ~50 wt% SiO₂ in the 150–200 MPa charges, whereas ~40 wt% in the 300–400 MPa samples (Table 3). Early fractionation of plagioclase and amphibole has already been recognized as a key process in generating alkaline liquids (Villemant et al., 2016), but the quasi-ubiquity of both phases in the experimental products does not allow deciphering the residual glass composition. Yet, biotite (low-silica phase) seems to be a major component driving the residual liquids towards high-silica low-alkali contents (sub-alkaline trend), whereas biotite-absent products show residual liquids following the alkaline trend. The lack of biotite in the Pavin magma may result from crystallization at low pressure (150–200 MPa), but also from relatively oxidized conditions (NNO+1.5) that favour clinopyroxene at the expense of biotite (Fig. 9a). Therefore, the pressure-driven crystallization sequence of a trachyandesitic melt deciphers the liquid line of descent, with major implications for alkaline versus sub-alkaline volcanic suites. Typically, the low-pressure biotite-lacking Pavin magma has a trachytic residual liquid, but it could have been different in case of crystallization at deeper levels in the stability field of biotite.

The trachytic residual liquid of the Pavin magma overlaps in major oxides with the trachytic whole rocks of the neighbouring Chaîne des Puys (Fig. 7; except that the Pavin glasses are enriched by ~1 wt% K₂O and depleted by ~1 wt% Na₂O compared to those of the Chaîne des Puys, which has been attributed to preferential fractionation of amphibole at the expense of clinopyroxene; Villemant et al., 2016). However, the accordance of the other oxides (and total alkali) makes possible the generation of trachytic liquids by main fractionation of amphibole, plagioclase, and clinopyroxene from a trachyandesitic parent in upper crustal conditions (<10 km), in agreement with previous mineralogical and geochemical studies on the Massif Central magmatic suites (e.g., Maury et al., 1980; Villemant et al., 1981). The trachyandesitic melts (such as the ones of the Pavin or Nugère for the Chaîne des Puys) may have fractionated early amphibole and plagioclase at upper crust level, but our experimental results bring the additional constraint that they did not fractionate significant biotite to produce trachytic residual liquids.

4. Conclusion

The Pavin pyroclasts are relatively heterogeneous in composition (crystal zonings, glomerocrysts, cumulates, etc.), which may result from two main processes: (i) a small volume of stored magma that makes it significantly sensitive to any physicochemical changes induced by deep magma recharge and (ii) an intermediate magma storage within the conduit (up to ~50 MPa; ~2.0 km in depth) that promotes crystallization of microlites, microphenocrysts, and phenocryst rims. Evaluating the phase assemblage and compositions that prevail in the reservoir, we infer magma storage conditions around 950–975 °C, 150–200 MPa (~5.5–7.0 km in depth), NNO+1.5, and 4.5–5.5 wt% melt H₂O. The residual liquids in equilibrium at these conditions are trachytic and compare to those of the neighbouring Chaîne des Puys trachytes (whole rock), making possible a differentiation trend by fractionation of at least 10–20 wt% of amphibole, plagioclase, and clinopyroxene. The experiments highlight the importance of crystallizing this assemblage at 150–200 MPa and out of the stability field of biotite to produce the trachytic liquids. In contrast, biotite plays a major role at 300–400 MPa in driving liquids towards sub-alkaline trends.

Acknowledgements

We thank Ida Di Carlo for assistance with SEM and EMP analyses, Rémi Champallier for assistance with the IHPV, and Michel Pichavant for fruitful discussions. This work is part of MR's undergraduate research project, which was partly funded by TLS Geothermics (France) and the French "Investissements d'avenir" Equipex_Planex Program (ANR-11-EQPX-0036; Bruno Scaillet). We greatly thank the reviewers for their useful suggestions that improved the manuscript.

Appendix A. Supplementary data

Supplementary data to this article can be found online at <https://doi.org/10.1016/j.crte.2019.07.003>.

References

- Ackerman, L., Ulrych, J., Řanda, Z., Erban, V., Hegner, E., Magna, T., Balogh, K., Frána, J., Lang, M., Novák, J., 2015. Geochemical characteristics and petrogenesis of phonolites and trachytic rocks from the České Středohoří volcanic complex, the Ohře Rift, Bohemian Massif. *Lithos* 224–225, 256–271.
- Arbaret, L., Bourdier, J.-L., 2018. Assessing the role of phreatomagmatism in the eruption dynamics of the trachyandesitic maar-like Pavin crater (Massif central, France): constraints from the pyroclasts microtextures. 7th International Maar Conference, Olot, Spain, *Abst. Vol.* pp. 18–19.
- Bacon, C.R., Hirschmann, M.M., 1988. Mg/Mn partitioning as a test for equilibrium between coexisting Fe–Ti oxides. *Am. Mineral.* 73, 57–61.
- Boivin, P., Besson, J.-C., Briot, D., Camus, G., de Goër de Herve, A., Gourgaud, A., Labazuy, P., Langlois, E.P., de Larouzière, F.D., Livet, M., Mergoil, J., Miallier, D., Morel, J.M., Vernet, G., Vincent, P., 2009. Volcanologie de la chaîne des Puys. Carte et fascicule. In: Parc naturel régional de la chaîne des Puys, 5^e ed., p. 200.
- Boivin, P., Besson, J.-C., Ferry, P., Gourgaud, A., Miallier, D., Thouret, J.-C., Vernet, G., 2010. Le point sur l'éruption du lac Pavin il y a 7 000 ans. *Rev. Sci. Nat. Auv.* 74–75, 45–56.
- Boivin, P., Miallier, D., Cluzel, N., Devidal, J.-L., Dousteyssier, B., 2015. Building and ornamental use of trachyte in the center of France

- during antiquity: sources and criteria of identification. *J. Archaeol. Sci.* 3, 247–256.
- Bourdier, J.-L., 1980. Contribution à l'étude volcanologique de deux secteurs d'intérêt géothermique dans le mont Dore : le groupe du Pavin et le massif du Sancy. PhD thesis. Université Clermont-Ferrand-2, France, p. 180.
- Briot, D., Cantagrel, J.-M., Dupuy, C., Harmon, R.S., 1991. Geochemical evolution in crustal magma reservoirs: trace-element and Sr–Nd–O isotopic variations in two continental intraplate series at Monts Dore, Massif Central, France. *Chem. Geol.* 89, 281–303.
- Brousse, R., 1961. Minéralogie et pétrologie des roches volcaniques du massif du Mont-Dore. *Bull. Soc. Fr. Mineral. Cristallogr.* 84 (131–186), 245–259.
- Camus, G., 1975. La chaîne des Puys (Massif central français) : étude structurale et volcanologique. PhD thesis. Université de Clermont-Ferrand-2, France.
- Camus, G., Goë de Herve, A., Kieffer, G., Mergoil, J., Vincent, P.M., 1973. Mise au point sur le dynamisme et la chronologie des volcans holocènes de la région de Besse-en-Chandesse (Massif central français). *C. R. Acad. Sci. Paris, Ser. D* 277, 629–632.
- Di Matteo, V., Carroll, M.R., Behrens, H., Vetere, F., Brooker, R.A., 2004. Water solubility in trachytic melts. *Chem. Geol.* 213, 187–196.
- Downes, H., 1984. Sr and Nd isotope geochemistry of coexisting alkaline magma series, Cantal, France. *Earth Planet. Sci. Lett.* 69, 321–334.
- Downes, H., 1987. Tertiary and Quaternary volcanism in the Massif Central, France. In: Fitton, J.C., Upton, B.G. (Eds.), *Alkaline Igneous Rocks*, 30. *Geol. Soc. Spec. Publ.*, pp. 517–530.
- Grove, T.L., Baker, M.B., 1984. Phase equilibrium controls on the tholeiitic versus calc-alkaline differentiation trends. *J. Geophys. Res.* 89 (B5), 3253–3274.
- Humphreys, M.C.S., Menand, T., Blundy, J.D., Klimm, K., 2008. Magma ascent rates in explosive eruptions: constraints from H₂O diffusion in melt inclusions. *Earth Planet. Sci. Lett.* 270, 25–40.
- Juvigné, E., Miallier, D., 2016. Distribution, tephrostratigraphy and chronostratigraphy of the widespread eruptive products of Pavin volcano. In: Sime-Ngando, T., Boivin, P., Chapron, E., Jézéquel, D., Meybeck, M. (Eds.), *Lake Pavin*. Springer Int. Publ., Switzerland, pp. 143–154.
- Leake, B.E., Woolley, A.R., Arps, C.E.S., Birch, W.D., Gilbert, C.M., Grice, J.D., Hawthorne, F.C., Kato, A., Kisch, H.J., Krivovichev, V.G., Linthout, K., Laird, J., Mandarin, J.A., Maresch, W.V., Nickel, E.H., Rock, N.M.S., Schumacher, J.C., Smith, D.C., Stephenson, N.C.N., Ungaretti, L., Whittaker, E.J.W., Youzhi, G., 1997. Nomenclature of amphiboles: report of the subcommittee on amphiboles of the international mineralogical association, commission on new minerals and mineral names. *Can. Mineral.* 35, 219–246.
- Le Bas, M.J., Le Maître, R.W., Streckeis, A., Zanettin, B., 1986. A chemical classification of volcanic rocks based on the total alkali-silica diagram. *J. Petrol.* 27, 745–750.
- Leyrit, H., Zylberman, W., Lutz, P., Jaillard, A., Lavina, P., 2016. Characterization of phreatomagmatic deposits from the eruption of the Pavin maar (France). In: Sime-Ngando, T., Boivin, P., Chapron, E., Jézéquel, D., Meybeck, M. (Eds.), *Lake Pavin*. Springer Int. Publ., Switzerland, pp. 105–128.
- Lustrino, M., Wilson, M., 2007. The circum-Mediterranean anorogenic Cenozoic igneous province. *Earth Sci. Rev.* 81 (1), 1–65.
- Martel, C., Champallier, R., Prouteau, G., Pichavant, M., Arbaret, L., Balcone-Boissard, H., Boudon, G., Boivin, P., Bourdier, J.-L., Scaillet, B., 2013. Phase relations in trachytes and implication for magma storage conditions in the Chaîne des Puys (French Massif Central). *J. Petrol.* 54 (6), 1071–1107.
- Maury, R., Brousse, R., Villemant, B., Joron, J.-L., Jaffrezic, H., Treuil, M., 1980. Cristallisation fractionnée d'un magma basaltique alcalin : la série de la chaîne des Puys (Massif central, France). I. Pétrologie. *Bull. Mineral.* 103, 250–266.
- Mollard, E., Martel, C., Bourdier, J.-L., 2012. Decompression-induced crystallization in hydrated silica-rich melts: empirical models of experimental plagioclase nucleation and growth kinetics. *J. Petrol.* 53 (8), 1743–1766.
- Putirka, K.D., 2008. Thermometers and barometers for volcanic systems. *Rev. Mineral. Geochem.* 69 (1), 61–120.
- Ridolfi, F., Renzulli, A., 2012. Calcic amphiboles in calc-alkaline and alkaline magmas: thermobarometric and chemometric empirical equations valid up to 1,130° C and 2.2 GPa. *Contrib. Mineral. Petrol.* 163 (5), 877–895.
- Sauerzapf, U., Lattard, D., Burchard, M., Engelmänn, R., 2008. The titanomagnetite–ilmenite equilibrium: new experimental data and thermo-oxybarometric application to the crystallization of basic to intermediate rocks. *J. Petrol.* 49 (6), 1161–1185.
- Schreiber, U., Anders, D., Koppen, J., 1999. Mixing and chemical interdiffusion of trachytic and latitic magma in a subvolcanic complex of the Tertiary Westerwald (Germany). *Lithos* 46 (4), 695–714.
- Ulrych, J., Pivec, E., Lang, M., Balogh, K., Kropacek, V., 1999. Cenozoic intraplate volcanic rock series of the Bohemian Massif: a review. *Geolines* 9, 123–129.
- Villemant, B., Joron, J.-L., Jaffrezic, H., Treuil, M., Maury, R., Brousse, R., 1980. Cristallisation fractionnée d'un magma basaltique alcalin : la série de la chaîne des Puys (Massif central, France). II. Géochimie. *Bull. Mineral.* 103, 267–286.
- Villemant, B., Jaffrezic, H., Joron, J.-L., Treuil, M., 1981. Distribution coefficients of major and trace elements, fractional crystallization in the alkali basalts of Chaîne des Puys (Massif Central, France). *Geochem. Cosmochim. Acta* 45, 1997–2022.
- Villemant, B., Caron, B., Thierry, P., Boivin, P., 2016. Magmatic evolution of Pavin's group of volcanoes: petrology, geochemistry and modeling of differentiation processes. In: Sime-Ngando, T., Boivin, P., Chapron, E., Jézéquel, D., Meybeck, M. (Eds.), *Lake Pavin*. Springer Int. Publ., Switzerland, pp. 129–140.
- Wilson, M., Downes, H., Cebria, J.-M., 1995. Contrasting fractionation trends in coexisting continental alkaline magmas series; Cantal, Massif Central, France. *J. Petrol.* 36, 1729–1753.
- Wörner, G., Beusen, J.M., Duchateau, N., Gijbels, R., Schmincke, H.U., 1983. Trace element abundances and mineral/melt distribution coefficients in phonolites from Laacher See Volcano (Germany). *Contrib. Mineral. Petrol.* 84, 152–173.